Original Article

The rationale for proposing a magnetic resonance slow diffusion metric and its proof-of-concept testing showing spleen parenchyma and hepatocellular carcinoma have faster diffusion than liver parenchyma

Fan-Yi Xu, Ben-Heng Xiao, Yì Xiáng J. Wáng^

Department of Imaging and Interventional Radiology, Faculty of Medicine, The Chinese University of Hong Kong, Hong Kong SAR, China

Contributions: (I) Conception and design: YXJ Wáng; (II) Administrative support: YXJ Wáng; (III) Provision of study materials or patients: YXJ Wáng; (IV) Collection and assembly of data: FY Xu, YXJ Wáng; (V) Data analysis and interpretation: FY Xu, BH Xiao, YXJ Wáng; (VI) Manuscript writing: All authors; (VII) Final approval of manuscript: All authors.

Correspondence to: Yì Xiáng J. Wáng, PhD. Department of Imaging and Interventional Radiology, Faculty of Medicine, The Chinese University of Hong Kong, 30-32 Ngan Shing Street, Shatin, New Territories, Hong Kong SAR, China. Email: yixiang_wang@cuhk.edu.hk.

Background: The liver and spleen have a similar amount of blood perfusion, and the spleen is waterier than the liver. The spleen tissue has a higher contrast-enhanced computed tomography (CT) extracellular volume fraction than the liver. The spleen has been reported to have a much lower apparent diffusion coefficient (ADC), intravoxel incoherent motion (IVIM)-perfusion fraction (PF), and IVIM-D_{slow} than those of the liver, which appears to be unreasonable. As hepatocellular carcinomas (HCCs) are mostly associated with increased blood supply and increased proportion of arterial blood supply and with edema, HCC has been reported to have a lower ADC, lower IVIM-PF, and lower IVIM-D_{slow} than liver parenchyma, which appears to be unreasonable. Cysts are known to have a longer T2 and a higher ADC than hemangiomas. Due to the 'flushing' of blood flow inside the hemangioma, we hypothesize that the actual diffusion of hemangioma liquid is faster than the more 'static' liquid of the cysts. As ADC measure is heavily affected by T2 and in order to minimize the T2 effect, we propose a new metric reflecting tissue slow diffusion which is termed 'slow diffusion coefficient (SDC)': $SDC = [S(b_1) - S(b_2)]/(b_2 - b_1)$, where b_1 and b_2 refers to a high b-value (e.g., 400 s/mm^2 for liver) and a higher b-value (e.g., 600 s/mm^2) respectively, where $S(b_1)$ and $S(b_2)$ denote the corresponding diffusion weighted image signal intensity.

Methods: This study utilized a random selection of authors' historical liver IVIM magnetic resonance imaging (MRI) data. For 1.5T data, SDC was calculated with b=600 and 800 s/mm^2 images. For 3.0T data, SDC was calculated with b=400 and 600 s/mm^2 images. With 1.5T data, SDC was calculated for 10 healthy volunteer cases' liver and spleen parenchyma, as well as two simple liver cysts and their corresponding liver parenchyma. With 3.0T data, SDC was calculated for 14 cases' liver and spleen parenchyma, as well as 13 HCC masses, 9 simple liver cysts, 13 hemangiomas and their corresponding liver parenchyma. As *in vivo* diffusion metrics can be only measured with MRI thus external validation is not possible, the measures of liver parenchyma were used to normalize the measures of spleen, HCC, cyst, and hemangioma, and the ratios were expressed in median value.

Results: The median ratio of SDC_{spleen}/SDC_{liver} was 2.47 for 1.5T data and 1.97 for 3.0T data. Two cysts at 1.5T had a median SDC_{cyst}/SDC_{liver} ratio of 2.92. For 3.0T data, the median ratios of SDC_{HCC}/SDC_{liver}, SDC_{cyst}/SDC_{liver}, $SDC_{hemangioma}/SDC_{liver}$ were 2.83, 4.23, and 5.37, respectively. However, the $ADC_{spleen}/$

^ ORCID: 0000-0001-5697-0717.

ADC_{liver} ratios were always <0.81 even when calculated with various combinations of high *b*-values.

Conclusions: The spleen has a faster diffusion than the liver, HCCs have a faster diffusion than the adjacent liver parenchyma, and hemangiomas have a faster diffusion than simple cysts. Although it is known that cysts have a substantially longer T2 than hemangiomas, SDC of hemangioma was higher than that of cysts, suggesting 'T2 effect' is minimized for SDC.

Keywords: Diffusion weighted imaging (DWI); liver; spleen; diffusion-derived vessel density (DDVD); slow diffusion coefficient (SDC)

Submitted Mar 03, 2025. Accepted for publication Mar 24, 2025. Published online Apr 10, 2025.
doi: 10.21037/qims-2025-537
View this article at: https://dx.doi.org/10.21037/qims-2025-537

Introduction

Diffusion weighted imaging (DWI) plays a pivotal role in magnetic resonance imaging (MRI) evaluation of a variety of pathologies. However, clinical application of the DWI derived quantitative metrics of apparent diffusion coefficient (ADC) and intravoxel incoherent motion (IVIM) parameters [perfusion fraction (PF), D_{slow}, D_{fast}] have not been very successful. ADC is indeed widely used, while it is generally regarded by physicians and radiologists that its role is only 'supportive' rather than 'confirmative'. IVIM technique has largely remained in the research phase.

In the literature reported *in vivo* ADC results, there exists a 'T2-ADC curve', with ADC measure strongly affected by T2 relaxation time (T2) (1-6). T2 can be divided into short T2 band [<60 millisecond (ms)], intermediate T2 band (60–80 ms), and long T2 band (>80 ms, all 3T values). For the short T2 time band, there is a negative correlation between T2 and ADC. For the long T2 time band, there is a positive correlation between T2 and ADC. A tissue likely measures a low ADC if its T2 is close to 70 ms (such as the cases of lymphoma, abscess liquid, and the acute phase of brain ischemic stroke). The spleen (with T2 of around 60 ms) and parotid gland Warthin' tumors (with T2 of around 80 ms) have a low ADC despite having rich blood perfusion. On the other hand, a tissue is likely to measure a high ADC if its T2 is far away from 70 ms, such as the cases of cartilage (with very short T2 and high ADC), myxoma and chondrosarcoma (both with very long T2 and very high ADC) (4). It appears to be unreasonable that the spleen has an ADC of only around 0.8×10^{-3} mm^2/s while chondrosarcoma has an ADC of around 2.3×10^{-3} mm^2/s (4). This 'T2-ADC curve' is graphically shown in *Figure 1* (2,4,5,7). Uterine myometrium has T2 and ADC similar to that of skeletal muscles (5). A synthetic analysis based on the articles of DeMulder *et al.* (8), Bura *et al.* (9), and Barral *et al.* (10) shows that, relative to the myometrium T2 and ADC, myometrium tumors with shorter T2 are associated with higher ADC, myometrium tumors with longer T2 are associated with lower ADC, and myometrium tumors with very longer T2 (cystic degenerated leiomyoma and myxoid degenerated leiomyoma) are associated with high ADC, thus being very consistent with the 'T2-ADC curve' [see the supplementary figure in (5)]. This high dependency of ADC on T2 suggests that, though ADC can be contributed to a certain degree by tissue diffusion, it is overall not a good biomarker to reliably reflect true tissue diffusion (6).

We have recently proposed the metric of diffusion derived 'vessel density' (DDVD) (11-13), which is derived from the equation:

$$DDVD_{b0b1} = S(b_0)/ROIarea0 - S(b_1)/ROIarea1 \quad [unit: arbitrary\ unit(au)/pixel] \quad [1]$$

where ROIarea0 and ROIarea1 refer to the number of pixels in the selected region of interest (ROI) on *b*=0 and *b*=1 s/mm^2 diffusion weighted (DW) image, respectively. $S(b_0)$ refers to the measured sum signal intensity within the ROI when *b*=0, and $S(b_1)$ refers to the measured sum signal intensity within the ROI when *b*=1 s/mm^2, thus $S(b)$/ROIarea equates to the mean signal intensity within the ROI. $S(b_1)$ and ROIarea1 can also be approximated by other low *b*-values (such as *b*=10 s/mm^2) DW image. We have demonstrated that, for the liver and spleen DDVD measurement, when the time of echo (TE) is short or modest and time of repetition (TR) is long (such as TR >1,600 ms, TE =60 ms) and the 2nd *b*-value is 1 or 2 mm^2/s, $DDVD_{liver}$ is approximately similar to $DDVD_{spleen}$ which agrees with the known physiology that liver and spleen have similar amount of blood perfusion (14). According to the

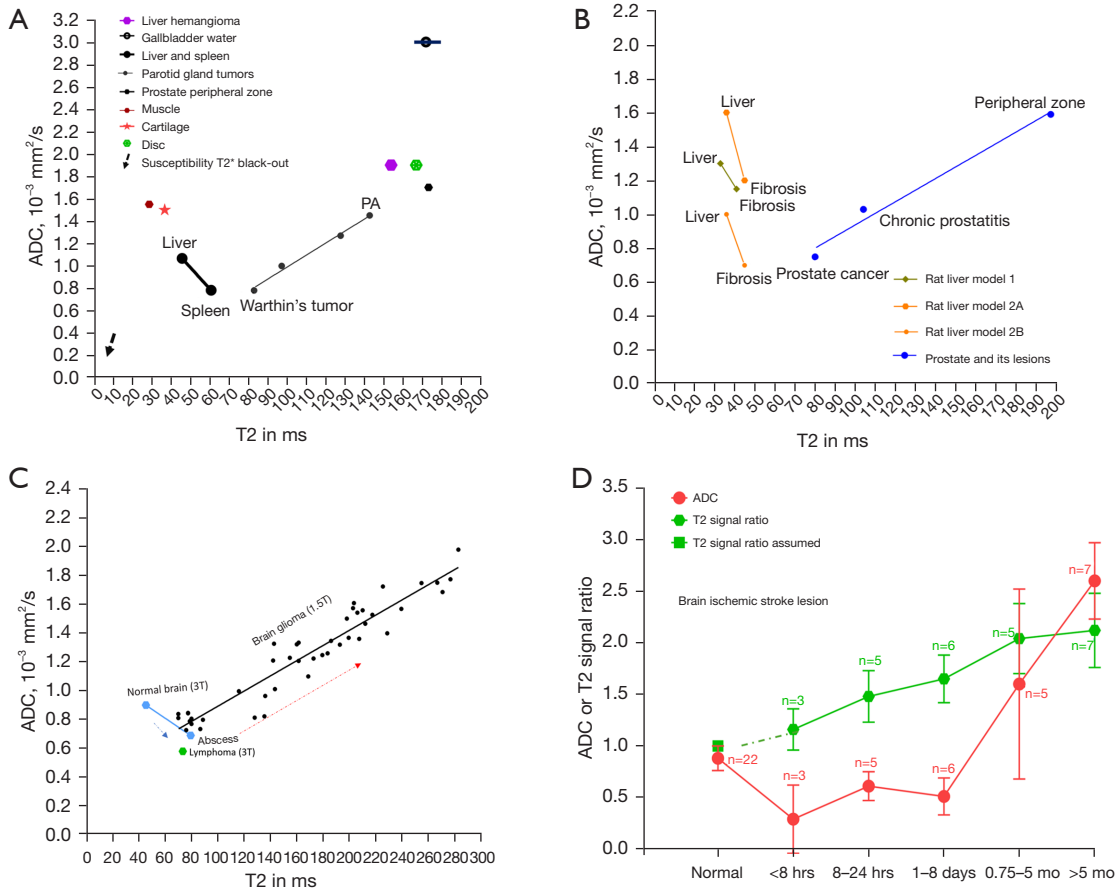

Figure 1 Data show triphasic dependency of ADC on T2 relaxation time. (A) and (B) are all 3.0T data. Only the liver fibrosis models in (B) are animal study results; all others are human study results. In (B), model 1 is with a partial bile duct ligation cholestatic liver fibrosis rat model, and ADC was based on *b*-values =0, 800 s/mm^2, model 2A (ADC based on *b*-values=0, 200 s/mm^2) and model 2B (ADC based on *b*-values =400, 500, 600, 800, 1,000 s/mm^2) are with a carbon tetrachloride liver fibrosis rat model. (A) is reused with permission from (4), (B) is adapted with permission from (2). (C) Triphasic dependency of ADC on T2 for brain tissues [reused with permission from (5)]. The dotted blue arrow shows that, as brain tissue turns into abscess or lymphoma, T2 increases and ADC decreases. The dotted red arrow shows that, as glioma T2 increases, glioma ADC increases. Data sources for (A-C) were explained in (2,4,5). (D) is based on brain ischemic stroke results reported by Lutsep *et al.* (7). Y-axis is ADC (×10^{-3} mm^2/s) or T2 signal ratio (ratio of stroke lesion signal intensity to normal brain signal intensity on T2-weighted image, and assumed to be 1 when without stroke). (D) indicates that, when T2 increases, ADC of the stroke lesion initially decreases and then increases, thus following a triphasic pattern. ADC, apparent diffusion coefficient; hrs, hours; mo, months; PA, pleomorphic adenoma.

analysis in (14), a liver DDVD value of 11 au/pixel at 1.5T or 35 au/pixel at 3.0T will be approximately equivalent to computed tomography (CT) perfusion of blood volume of 18 mL/100 mL with a blood flood speed of around 1.2 mL/min/mL. This also correlates with the liver IVIM-PF measure of about 18% reported by us (15). In physiological studies, the hepatic blood volume including that of the large vessels is about 25 mL/100 g and blood flow is about 1.04 mL/min/mL (16). When a TE of 59 ms (TR =1,600 ms, free breathing acquisition) and *b*=0, 2 mm^2/s were used for the DDVD calculation of 26 cases of hepatocellular carcinoma (HCC), we measured a mean $DDVD_{HCC}/DDVD_{liver}$ ratio of 1.42. This value agrees well with the perfusion CT blood volume literature results median ratio of 1.38, while the perfusion CT blood flow literature results mean ratio is 1.92 (*Figure 2*) (17). Our study of parotid tumor DDVD also showed parotid tumor DDVD ratio measures were consistent with CT measured

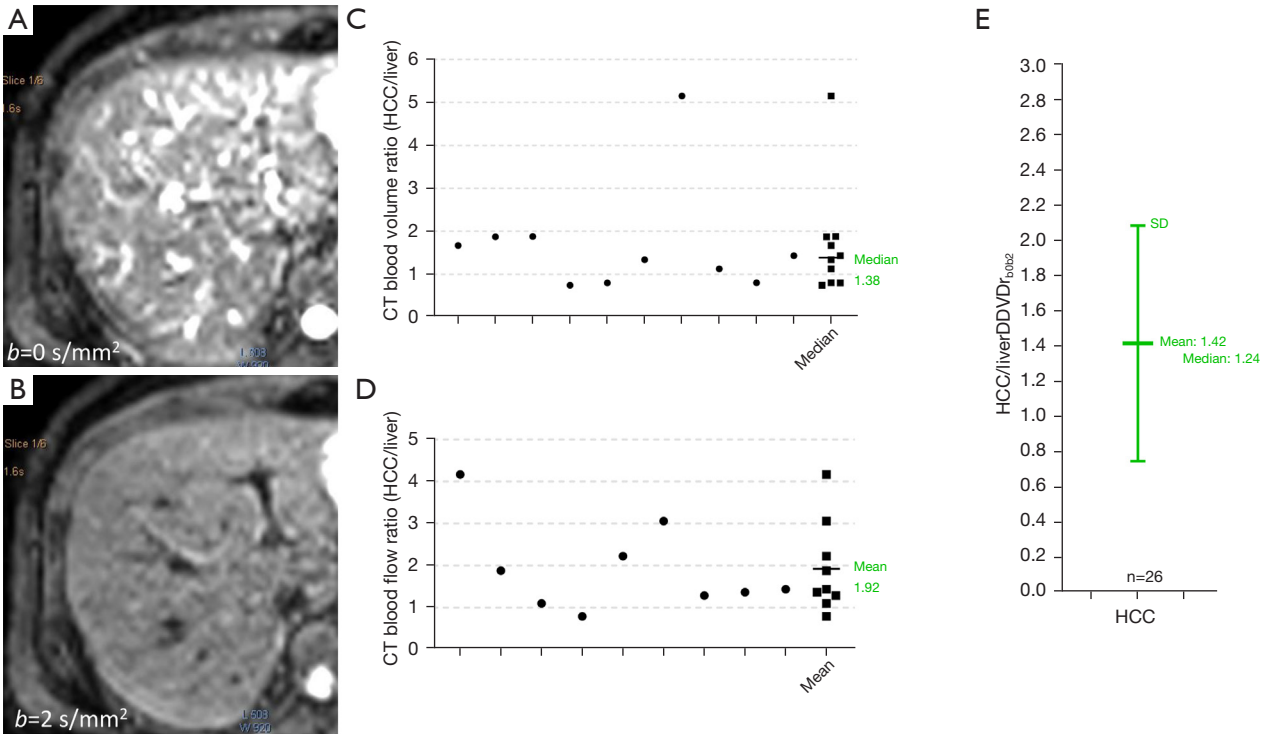

Figure 2 The $DDVD_{HCC}/DDVD_{liver}$ ratio agrees well with the HCC/liver ratio of perfusion CT measured blood volume. (A,B) 1.5T liver diffusion weighted images with *b*-value of 0 (A), 2 s/mm^2 (B). The signal difference between *b*=0 s/mm^2 image and *b*=2 s/mm^2 images is dramatic, particularly the vessels show high signal when the motion probing gradient is 'off' while show dark signal when the motion probing gradient is 'on'. The high intensity of the vasculature seen on *b*=0 s/mm^2 image, which is different from conventional T2-weighted image and suggests an 'angiographic effect', led to the naming of DDVD. (C,D) HCC measure to surround liver parenchyma measure ratios of perfusion CT measured blood volume (C) and blood flow speed (D). (C,D) are based on a random selection of 10 reports for blood volume and 9 reports for blood flow speed (each dot represents the result from one study, except the dots for median/mean value calculation). (E) is based on authors' own data of 26 cases of HCC. DDVDr was measured at 3.0T, with a TE of 59 ms (TR =1,600 ms, free breathing acquisition) and *b*=0, 2 s/mm^2. This figure is reused with permission from (17). CT, computed tomography; DDVD, diffusion derived 'vessel density'; DDVDr, DDVD ratio; HCC, hepatocellular carcinoma; SD, standard deviation; TR, time of repetition; TE, time of echo.

blood volume ratios (18). One of the initial goals of using DDVD was to minimize the T2 effect (which is defined as MRI signal differences contributed by T2 relaxation time difference). This is approximately achieved when TR is long and TE is short or modest (17). DDVD is less sensitive to TE selection and the 'T2 effect' compared to that of ADC and IVIM (17).

As *in vivo* diffusion metrics can be only measured with MRI thus external validation is not possible for diffusion metrics, it will be convenient and practical for us to consider liver/spleen parenchyma as the reference tissues. The spleen has been known to have a much lower ADC than the liver. However, the liver and spleen have similar amounts of blood perfusion per tissue volume per minute (14), and the spleen is waterier than the liver (the spleen has longer T1 and longer T2 than the liver, and the spleen has lower CT density than the liver). The magnetization transfer signal ratio (MTR) measure shows a higher proportion of water molecules in the liver are bound to other macromolecules than the water molecules in the spleen (19), which supports that water molecules in the spleen have a greater extent of free diffusion. Free water molecules also allow longer T1 and T2 relaxation times than bounded water molecules. The spleen is also an organ with the function of storing blood (20). The spleen can respond to sympathetic stimulation by contracting its fibroelastic capsule and trabeculae to increase systemic blood supply. Recently, Yeung *et al.* (21) reported that spleen tissue had a

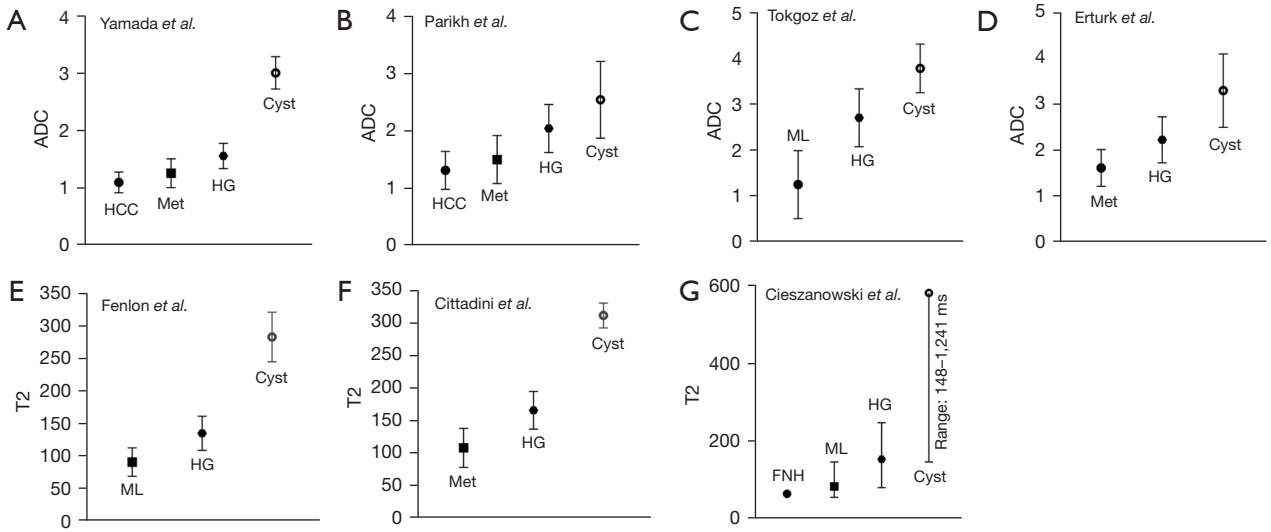

Figure 3 Compared to simple liver cyst, the liver HG has a substantially shorter T2 and a substantially lower ADC. Data are re-plotted from the reports of Yamada *et al.* (22), Parikh *et al.* (23), Tokgoz *et al.* (24), Erturk *et al.* (25), Fenlon *et al.* (26), Cittadini *et al.* (27), and Cieszanowski *et al.* (28). (A-F) Data in mean ± standard deviation; (G) data in mean and range. Y-axis: ADC in $\times 10^{-3}$ mm^2/s or T2 in millisecond (ms). ADC, apparent diffusion coefficient; FNH, focal nodular hyperplasia; HCC, hepatocellular carcinoma; HG, hemangioma; Met, metastases; ML, malignant lesions.

higher contrast-enhanced CT extracellular volume fraction (ECV) than the liver, in healthy tissues and in tissues with systemic amyloid light-chain amyloidosis. We consider that it is unreasonable that spleen ADC is much lower than liver ADC. As HCCs are mostly associated with increased blood supply and increased proportion of arterial blood supply and higher water content (i.e., edema, as shown with higher signal on T2-weighted image and with lower density on X-ray CT), we consider that it is also unreasonable that HCC has a lower ADC than adjacent liver parenchyma. We argue that the lower ADC of the spleen and HCC relative to liver parenchyma is due to their longer T2 relative to liver parenchyma (6).

Another two entities with confusing ADC measures are liver hemangioma and simple liver cyst. Cysts are known to have a longer T2 and a higher ADC than hemangioma (*Figure 3*) (22-28). We also hypothesize that the higher ADC of liver simple cysts are due to their longer T2 (6). Due to the 'flushing' of blood flow inside the hemangioma, we hypothesize that actual diffusion of hemangioma liquid is faster than the more 'static' liquid of the cysts. Indeed, in a gadolinium-enhanced dynamic MRI study, Nam *et al.* (29) reported that ADC values were higher in the rapidly contrast enhancing hemangiomas than in the intermediately or the slowly contrast enhancing hemangiomas.

During the course of our research activities and following the same concept as DDVD, we found that we can use a straightforward method to calculate a metric reflecting tissue slow diffusion, and we term this metric as 'slow diffusion coefficient (SDC)':

$$SDC = \frac{S(b_1) - S(b_2)}{b_2 - b_1} \left[unit: au/s\right] \quad [2]$$

where b_1 and b_2 refers to a high *b*-value (e.g., 400 mm^2/s for the case of liver DWI) and a higher *b*-value respectively (e.g., 600 mm^2/s for the case of liver DWI), where S(b_1) and S(b_2) denote the image signal intensity acquired at the high *b*-value and the higher *b*-value respectively (*Figure 4*). In this study, we explain the rationale of why we propose such a diffusion metric and attempt to conduct proof-of-concept testing with the liver, spleen, HCC, liver hemangioma, and simple liver cysts for such a metric. As ADC measure is heavily affected by T2 (6), we test whether SDC can minimize the T2 effect.

Methods

This is a retrospective analysis of previously prospectively acquired liver IVIM data. The study was conducted in

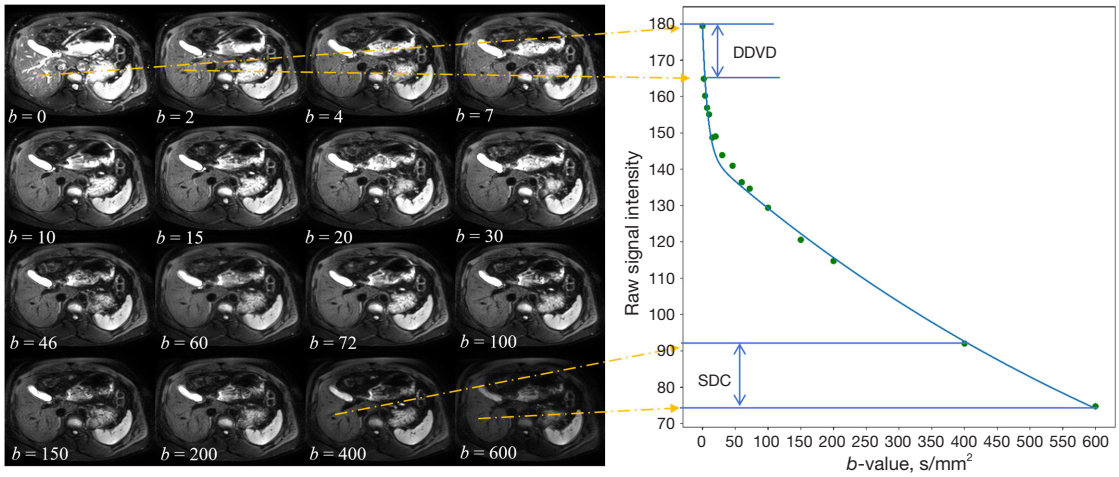

Figure 4 The images on the left are one liver IVIM series with various *b*-values. The graph on the right is the corresponding signal decay curve for the liver. As *b*-value increases, the liver signal intensity decreases on DW images, and the data are fitted with a bi-exponential decay model (blue curve line). We use the initial fast signal decay (e.g., *b*=0 and *b*=2 s/mm^2 data) to calculate DDVD and use the later part with high values (such as *b*=400 and *b*=600 s/mm^2 data) to calculate SDC. DDVD, diffusion derived vessel density; DW, diffusion weighted; IVIM, intravoxel incoherent motion; SDC, slow diffusion coefficient.

accordance with the Declaration of Helsinki (as revised in 2013). All IVIM data were acquired with institutional ethical approval and with informed consent obtained from individual participants. 1.5T MRI was performed with a Philips scanner (Achieva, Philips Healthcare, Best, Netherlands). The IVIM diffusion imaging was based on a single-shot spin-echo type echo-planar sequence, with 15 *b*-values of 0, 1, 2, 15, 20, 30, 45, 50, 60, 80, 100, 200, 300, 600, and 800 s/mm^2. Number-of-excitation (NEX) was 2 for all image acquisition. The TR was 1,600 ms and the TE was 63 ms. SPIR technique (Spectral Pre-saturation with Inversion-Recovery) was used for fat suppression. Respiratory-gating was applied in all scan participants. Other parameters included slice thickness =7 mm and inter-slice gap 1 mm, matrix =124×97, field of view (FOV) =375 mm × 302 mm, number of slices =6. 3.0T MRI was performed with a Philips scanner (Ingenia, Philips Healthcare, Best, Netherlands). The IVIM diffusion imaging was based on a single-shot spin-echo type echo-planar sequence, with 16 *b*-values of 0 (NEX =5), 2 (NEX =5), 4 (NEX =1), 7 (NEX =1), 10 (NEX =1), 15 (NEX =1), 20 (NEX =1), 30 (NEX =1), 46 (NEX =1), 60 (NEX =3), 72(NEX =1), 100 (NEX =1), 150 (NEX =1), 200 (NEX =1), 400 (NEX =2), and 600 (NEX =2) s/mm^2. The default SPIR technique was used for fat suppression. The TR was 1,600 ms and the TE was 59 ms. Data was acquired with free breathing. Other parameters included slice thickness =7 mm and inter-slice gap =1.5 mm, matrix =123×124, FOV =372 mm × 341 mm, number of slices =20.

All image processing was implemented in a custom program developed on MATLAB (Mathworks, Natick, MA, USA). For the analysis of liver and spleen parenchyma, on each DW image for the liver/spleen, ROIs were drawn to cover a large portion of the right liver parenchyma and spleen parenchyma while avoiding large vessels and artifacts. Based on Eq. [1], for 1.5T data, $DDVD_{b0b1}$, $DDVD_{b0b2}$, $DDVD_{b0b15}$, $DDVD_{b0b20}$, and $DDVD_{b0b30}$, $DDVD_{b0b45}$, $DDVD_{b0b50}$, $DDVD_{b0b60}$, $DDVD_{b0b80}$, $DDVD_{b0b100}$, $DDVD_{b0b200}$, $DDVD_{b0b300}$, $DDVD_{b0b600}$, and $DDVD_{b0b800}$, were calculated from *b*=0 and *b*=1, *b*=0 and *b*=2, *b*=0 and *b*=15, *b*=0 and *b*=20, *b*=0 and *b*=30, *b*=0 and *b*=45, *b*=0 and *b*=50, *b*=0 and *b*=60, *b*=0 and *b*=80, *b*=0 and *b*=100, *b*=0 and *b*=200, *b*=0 and *b*=300, *b*=0 and *b*=600, and *b*=0 and *b*=800 s/mm^2 images, respectively. For 3.0T data, $DDVD_{b0b2}$, $DDVD_{b0b4}$, $DDVD_{b0b7}$, $DDVDb_{0b10}$, $DDVD_{b0b15}$, $DDVD_{b0b20}$, and $DDVD_{b0b30}$, $DDVD_{b0b46}$, $DDVD_{b0b60}$, $DDVD_{b0b72}$, $DDVD_{b0b100}$, $DDVD_{b0b150}$, $DDVD_{b0b200}$, $DDVD_{b0b400}$, and $DDVD_{b0b600}$, were calculated from *b*=0 and *b*=2, *b*=0 and *b*=4, *b*=0 and *b*=7, *b*=0 and *b*=10, *b*=0 and *b*=15, *b*=0 and *b*=20, *b*=0 and *b*=30, *b*=0 and *b*=46, *b*=0 and *b*=60, *b*=0 and *b*=72, *b*=0 and *b*=100, *b*=0 and *b*=150, *b*=0 and *b*=200, *b*=0 and *b*=400, and *b*=0 and *b*=600 s/mm^2 images, respectively.

For 1.5T data, $SDC_{b600b800}$ was calculated according

to Eq. [2], where b_2 and b_1 refer to 800 and 600 s/mm^2, respectively, and S(b_2) and S(b_1) denote the signal intensity on b=800 and b=600 s/mm^2 images, respectively. For 3.0T data, $SDC_{b400b600}$ was calculated according to Eq. [2], where b_2 and b_1 refer to 600 and 400 s/mm^2, respectively, and S(b_2), and S(b_1) denote the signal intensity on b=600 and on b=400 s/mm^2 images, respectively. With 1.5T data, $SDC_{b600b800}$ was calculated for 10 healthy volunteer cases' liver and spleen parenchyma, as well as two simple liver cysts and their corresponding liver parenchyma. With 3.0T data, $SDC_{b400b600}$ was calculated for 14 healthy volunteer cases' liver and spleen parenchyma, as well as 13 HCC masses, 9 simple liver cysts, 13 hemangiomas and their corresponding liver parenchyma. These HCC, hemangioma, and cysts happened to exist in our datasets, and a random selection for these lesions was only based on that they were of reasonable sizes for measurement. Measurement of HCC excluded apparent necrotic areas whenever possible.

Based on the ROI drawn for DDVD analysis, conventional ADC was calculated according to:

$$ADC = \frac{\ln\left(S(b_1)/S(b_2)\right)}{b_2 - b_1}\left[unit: mm^2/s\right] \quad [3]$$

where b_2 and b_1 refers to the high b-value and low b-value respectively, where S(b_2) and S(b_1) denote the image signal intensity acquired at the high b-value and low b-value respectively.

Based on Eq [3], for 1.5T data, ADC_{b1b800}, ADC_{b2b800}, $ADC_{b15b800}$, $ADC_{b20b800}$, and $ADC_{b30b800}$, $ADC_{b45b800}$, $ADC_{b50b800}$, $ADC_{b60b800}$, $ADC_{b80b800}$, $AD_{b100b800}$, $ADC_{b200b800}$, $ADC_{b300b800}$, and $ADC_{b600b800}$, were calculated from b=1 and b=800, b=2 and b=800, b=15 and b=800, b=20 and b=800, b=30 and b=800, b=45 and b=800, b=50 and b=800, b=60 and b=800, b=80 and b=800, b=100 and b=800, b=200 and b=800, b=300 and b=800, and b=600 and b=800 s/mm^2 images, respectively. For 3.0T, ADC_{b2b600}, ADC_{b4b600}, ADC_{b7b600}, $ADC_{b10b600}$, $ADC_{b15b600}$, $ADC_{b20b600}$, and $ADC_{b30b600}$, $ADC_{b46b600}$, $ADC_{b60b600}$, $ADC_{b72b600}$, $ADC_{b100b600}$, $ADC_{b150b600}$, $ADC_{b200b600}$, and $ADC_{b400b600}$, were calculated from b=2 and b=600, b=4 and b=600, b=7 and b=600, b=10 and b=600, b=15 and b=600, b=20 and b=600, b=30 and b=600, b=46 and b=800, b=60 and b=600, b=72 and b=600, b=100 and b=600, b=150 and b=600, b=200 and b=600, and b=400 and b=600 s/mm^2 images, respectively.

For each case, the mean signal intensity of each ROI was weighted by the number of pixels included in each ROI in different slices, then the average of the weighted DDVDs was calculated to obtain the value for each case. The measures of liver parenchyma were used to normalize the measures of spleen parenchyma, HCC, cysts, and hemangiomas. Data are presented graphically. For statistics, SDC values were tested by Mann-Whitney U test. A P value <0.05 was considered statistically significant, >0.1 as not significant, and between 0.05 and 0.1 as with a trend of significance.

Results

The $DDVD_{spleen}/DDVD_{liver}$ ratio results with the 2nd b-value started being very low and increased to 800 s/mm^2 for 1.5T data and 600 s/mm^2 for 3.0T are shown in *Figure 5*. For 1.5T's $DDVD_{b0b1}$, the ratio of $DDVD_{spleen}/DDVD_{liver}$ was 1.24; from $DDVD_{b0b15}$ to $DDVD_{b0b80}$, the ratio of $DDVD_{spleen}/DDVD_{liver}$ stayed around or slightly below 1. For 3.0T, from $DDVD_{b0b2}$ to $DDVD_{b0b100}$, the ratio of $DDVD_{spleen}/DDVD_{liver}$ stayed around or slightly below 1. From $DDVD_{b0b100}$ to $DDVD_{b0b800}$ for 1.5T and from $DDVD_{b0b150}$ to $DDVD_{b0b600}$ for 3.0T, $DDVD_{spleen}/DDVD_{liver}$ ratio became increasingly higher.

The ratios of SDC_{spleen}/SDC_{liver} and SDC_{cyst}/SDC_{liver} for 1.5T data are shown in *Figure 6A*, and the ratios of SDC_{spleen}/SDC_{liver}, SDC_{HCC}/SDC_{liver}, SDC_{cyst}/SDC_{liver}, and $SDC_{hemangioma}/SDC_{liver}$ for 3.0T data are shown in *Figure 6B*. For both 1.5T and 3.0T data, SDC_{spleen}/SDC_{liver} was >1, and a trend was noted with '$SDC_{hemangioma}/SDC_{liver}$' > '$SDC_{cyst}/SDC_{liver}$' > '$SDC_{HCC}/SDC_{liver}$' > '$SDC_{spleen}/SDC_{liver}$'. Absolute SDC values of the above data are shown in *Figure 7*, with the hemangiomas having the highest median SDC value. Parametric visualizations of these results are shown in *Figures 8-11*.

ADC_{spleen}/ADC_{liver} ratio from ADC_{b1b800} to $ADC_{b600b800}$ for 1.5T data and from ADC_{b2b600} to $ADC_{b400b600}$ for 3.0T data are shown in *Figure 12*, with all the ratio values being <0.81.

Discussion

The results in *Figure 5* show the change of DDVD values following the increase of the 2nd b-value. Note that, an application of the diffusion gradients will lead to a decrease in observed T2 for tissues, which can be interpreted as an application of diffusion gradients is associated with a longer TE for data acquisition (30,31). Our modeling analysis shows that, when the 2nd b-value is very low (such as 1 s/mm^2), liver and spleen DDVD measures are contributed by both blood pool volume and blood flow speed; however, when

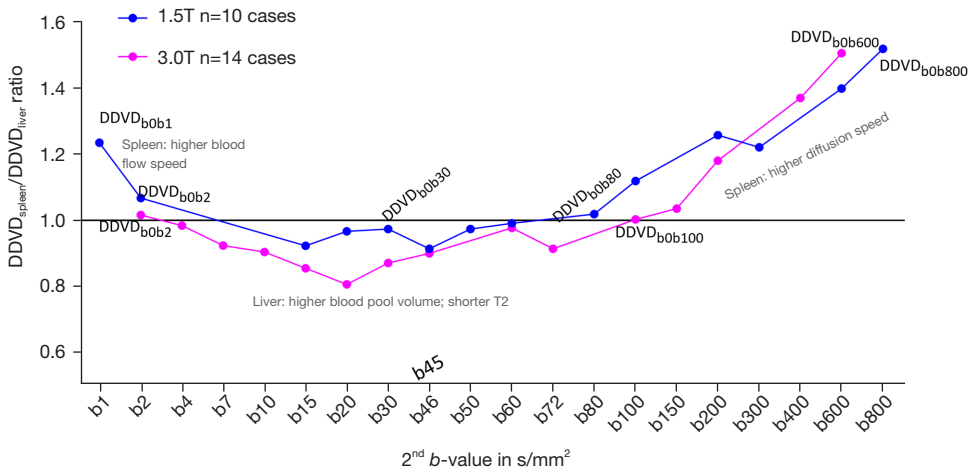

Figure 5 DDVD$_{spleen}$/DDVD$_{liver}$ ratio results from DDVD$_{b0b1}$ to DDVD$_{b0b800}$ for 1.5T and from DDVD$_{b0b2}$ to DDVD$_{b0b600}$ for healthy volunteers. The 2nd *b*-value starts from 1 s/mm^2 for 1.5T and 2 s/mm^2 for 3.0T and then increases to 800 s/mm^2 for 1.5T and 600 s/mm^2 for 3.0T. There is an initial slight decrease and then followed by a substantial increase in DDVD$_{spleen}$/DDVD$_{liver}$ ratio, and the changes in trend are more noticeable with 3.0T data than 1.5T data. See first paragraph in discussion for the explanation of the trends seen in this graph. Note that TE for was 63 ms for 1.5T acquisition and 59 ms for 3.0T acquisition. DDVD, diffusion derived vessel density.

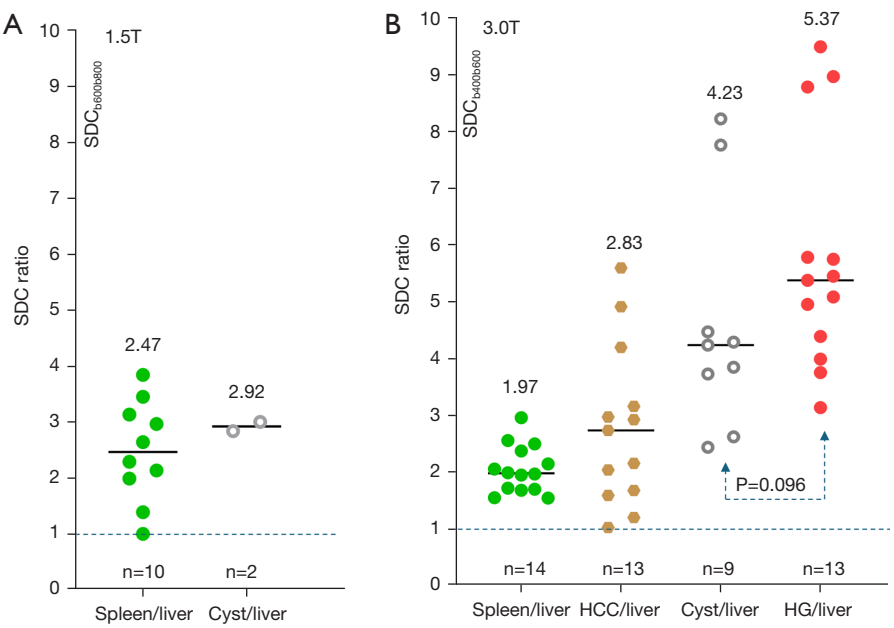

Figure 6 SDC ratio results for spleen/liver (healthy volunteer), cyst/liver, HCC/liver, and HG/liver. (A) 1.5T results; (B) 3.0T results. All the ratios have a median value >1. The ratio values for liver lesions are scattered, partly due to some of the lesion sizes being small. HCC, hepatocellular carcinoma; HG, hemangioma; SDC, slow diffusion coefficient.

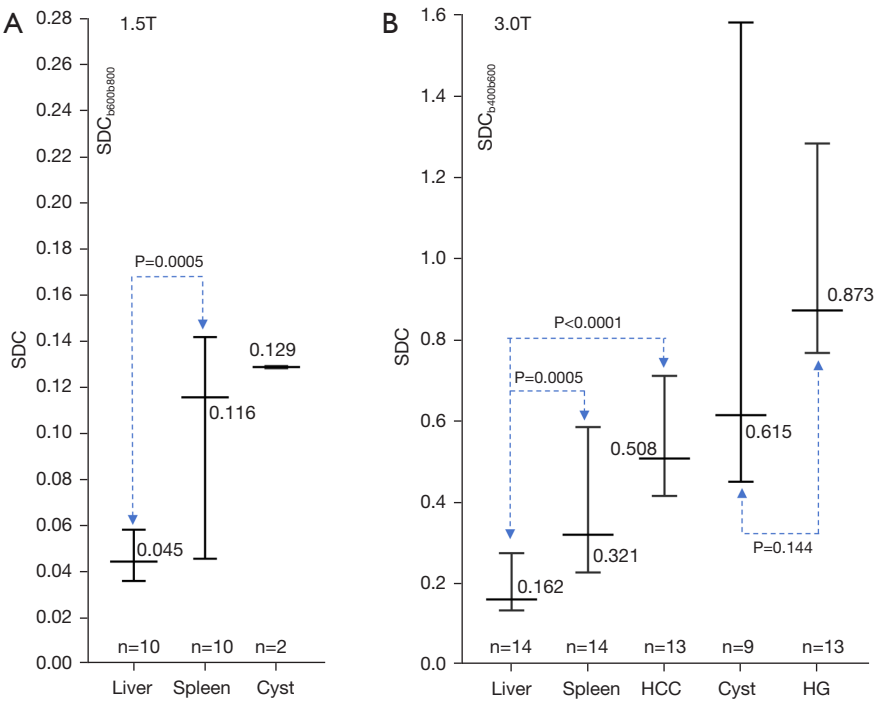

Figure 7 SDC absolute values (au/s, median and 95% confidence level) for the liver (healthy volunteer), spleen (healthy volunteer), cyst, HCC, and HG. (A) 1.5T results for $SDC_{b600b800}$; (B) 3.0T results for $SDC_{b400b600}$. The large 95% confidence level for liver lesions is partly due to some of the lesion sizes being small. HCC, hepatocellular carcinoma; HG, hemangioma; SDC, slow diffusion coefficient.

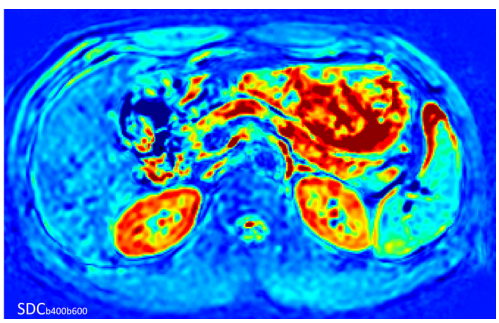

Figure 8 A SDC pixel map (calculated by b=400 and b=600 s/mm^2) of upper abdomen showing the SDC value for spleen is higher than the SDC value for liver. Also note that the kidneys show very high SDC value. Data were acquired at 3.0T. SDC, slow diffusion coefficient.

the 2nd b-value is only low (such as 10 or 20 s/mm^2), then liver and spleen DDVD measures are more contributed by blood pool volume (13). It has been reviewed that the blood pool volume of the liver is slightly larger than that of the spleen, while the blood flow speed of the spleen is slightly faster than that of the liver [see *Tab. 1* and *Tab. 2* in (14)]. *Figure 5* shows that, when the 2nd b-value was 1 s/mm^2, $DDVD_{spleen}/DDVD_{liver}$ was slightly larger than 1. When the 2nd b-value was between >2 and 100 s/mm^2, a shorter T2 of the liver than that of the spleen (liver T2 =40 ms, spleen T2 =60 ms, 3.0T data) might have led to a faster initial signal decay during DWI signal acquisition and promotes '*fast compartment*' measurement (6,31), and with these 2nd b-value ranges, $DDVD_{spleen}/DDVD_{liver}$ was around 0.9 (*Figure 5*). This remains also reasonable since liver blood pool volume is indeed slightly larger than that of the spleen. Following the 2nd b-value being higher and higher, liver and spleen DDVD values were contributed more and more by slow diffusion (13). $DDVD_{spleen}/DDVD_{liver}$ ratio returned to 1 when the 2nd b-value was around 80 s/mm^2 for 1.5T and around 100 s/mm^2 for 3.0T. After the 2nd b-value was ≥150 s/mm^2, the slow diffusion's contribution to DDVD further built up, and the measure for spleen became higher than the measure for liver. According to the IVIM theory, the perfusion contribution would already have been very small at the stage when the 2nd b-value is ≥150 s/mm^2. In addition, since liver and spleen have similar amounts of perfusion, data in *Figure 5* show that when the 2nd b-value

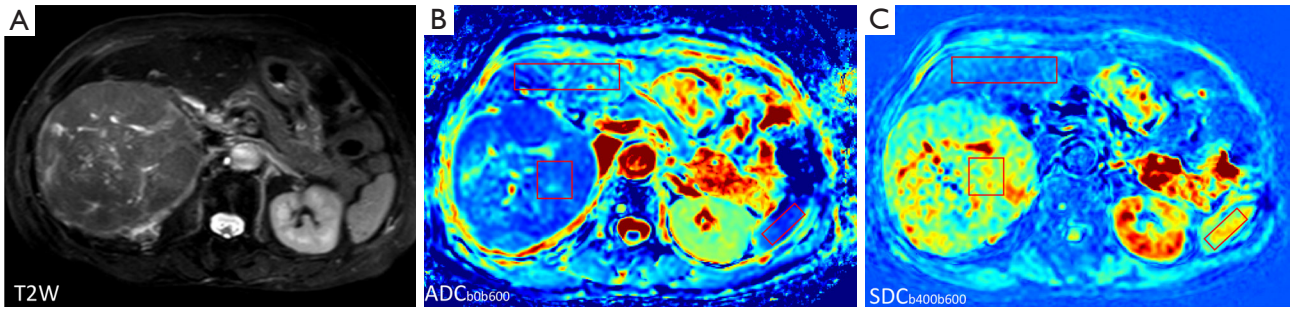

Figure 9 HCC tumorous tissue shows higher SDC than adjacent liver parenchyma. (A) is a T2W image, where the HCC mass shows substantially higher signal compared with the surrounding liver tissue, indicating edema of the HCC. The spleen also shows higher signal compared to the liver, indicating that the water content of the spleen is higher. (B) is an ADC pixel map (calculated with b=0 and b=600 s/mm^2 images) showing that the ADC values of HCC and spleen are lower than that of liver parenchyma. (C) is an SDC pixel map (calculated with b=400 and b=600 s/mm^2 images) showing SDC values of HCC and spleen are higher than that of liver parenchyma. With tissues in the boxes measured (square for the HCC, large rectangle for liver parenchyma, and small rectangle for spleen parenchyma), the results are: ADC_{HCC}/ADC_{liver} =0.822, ADC_{spleen}/ADC_{liver} =0.811, SDC_{HCC}/SDC_{liver} =5.48, SDC_{spleen}/SDC_{liver} =6.11. Data were acquired at 3.0T. The color scale may differ among the images, as the goal of illustration is to use the liver parenchyma as reference. ADC, apparent diffusion coefficient; HCC, hepatocellular carcinoma; SDC, slow diffusion coefficient; T2W, T2-weighted.

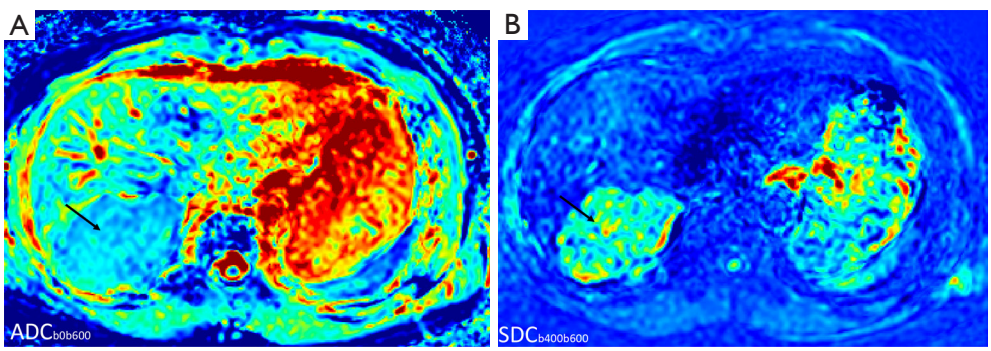

Figure 10 HCC tumorous tissue (arrow) shows lower ADC and higher SDC than adjacent liver parenchyma. (A) ADC pixel map (calculated with b=0 and b=600 s/mm^2 images). (B) SDC pixel map (calculated with b=400 and b=600 s/mm^2 images). Data were acquired at 3.0T. The color scale may differ among the images, as the goal of illustration is to use the liver parenchyma as reference. ADC, apparent diffusion coefficient; HCC, hepatocellular carcinoma; SDC, slow diffusion coefficient.

was sufficiently large, slow diffusion started to dominate the DDVD value resulting in $DDVD_{spleen}$ being measured higher than $DDVD_{liver}$. Such a DDVD observation suggests that it is possible to predominately measure the slow diffusion, and thus the conceiving of the SDC metric (*Figure 4*). In *Figure 5*, the changes of the trends were more 'substantial' for 3.0T data than for 1.5T data. This is likely due to that the T2 relaxation times were shorter at 3.0T than at 1.5T.

In this study, as shown in *Figures 6*,*7*, we confirmed that SDC_{spleen} was higher than SDC_{liver}. This is consistent with the fact that spleen has a higher extent of free water (thus likely with a faster slow diffusion than that of the liver). We also confirmed that SDC_{HCC} was higher than SDC_{liver}, and this agrees with the facts that HCC tumorous tissue has a higher water extent, being higher perfused and being perfused mainly with arterial blood (while liver parenchyma is perfused about 3/4 with venous blood). Another interesting observation is that $SDC_{hemangioma}$ is higher than SDC_{cyst}. Earlier literature reported substantially higher ADCs for cysts than for hemangiomas (*Figure 3*). Due to the 'flushing' of blood flow inside the hemangioma, it is reasonable that the diffusion of hemangiomas liquid is

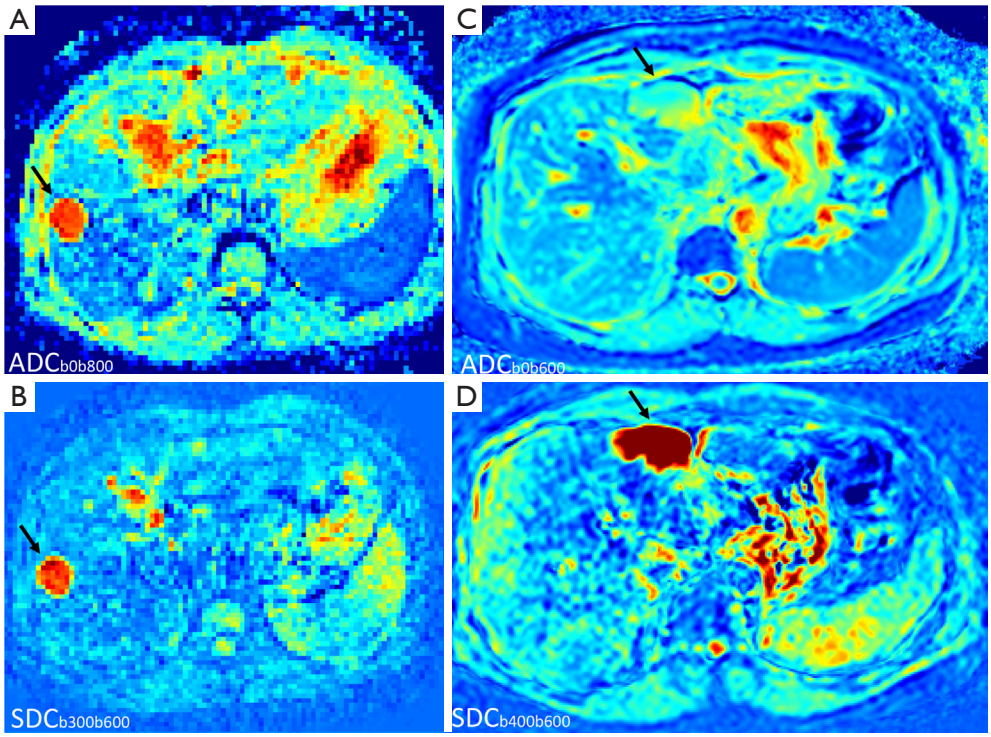

Figure 11 Case examples show that $SDC_{hemangioma}/SDC_{liver}$ ratio is higher than SDC_{cyst}/SDC_{liver} ratio. (A,B) A liver cyst (arrow); (C,D) a liver hemangioma (arrow). (A,C) ADC pixel map; (B,D) SDC pixel map. Compared with the background liver, the SDC of the cyst is also with high signal (B), but the relative signal is even higher on the ADC map (A). Compared with the background liver, the ADC of the hemangioma is also with high signal (C), but the relative signal is even higher on the SDC map (D). Cyst images (A,B) were acquired at 1.5T; hemangioma images (C,D) were acquired at 3.0T. The color scale may differ among the images, as the goal of illustration is to use the liver parenchyma as reference. ADC, apparent diffusion coefficient; SDC, slow diffusion coefficient.

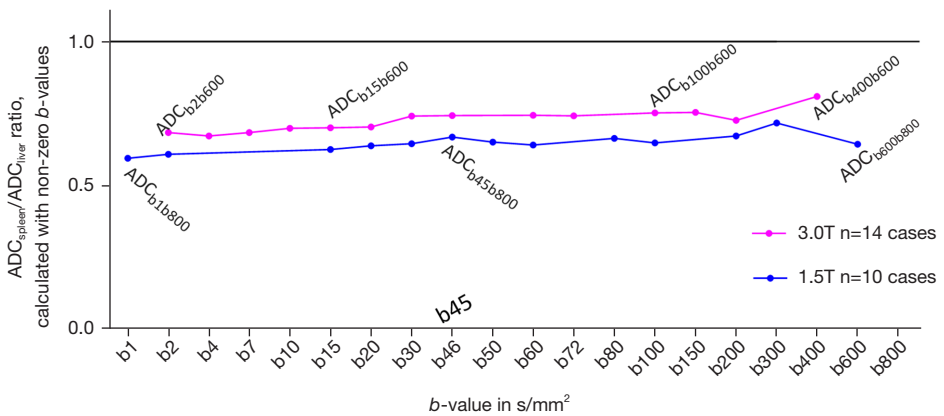

Figure 12 ADC_{spleen}/ADC_{liver} ratio results from ADC_{b1b800} to $ADC_{b600b800}$ for 1.5T and from ADC_{b2b600} to $ADC_{b400b600}$ for 3.0T for healthy volunteers. The higher *b*-value is always 800 s/mm^2 for 1.5T data and 600 s/mm^2 for 3.0T data. The 1st *b*-value starts from 1 s/mm^2 for 1.5T and 2 s/mm^2 for 3.0T and then increases to 600 s/mm^2 for 1.5T and 400 s/mm^2 for 3.0T. All the ratio values are <0.81. ADC, apparent diffusion coefficient.

faster than that of the more 'static' liquid of the cysts. Note that, the size of a water molecule is 280 picometers. If we consider that the size of a hepatocyte is 25 μm in diameter, then the size ratio of water molecule to hepatocyte is about 1/100,000. If we consider that the size of a spleen cell is 6.5 μm in diameter, then the size ratio of water molecule to spleen cell is about 1/26,000. Hepatic sinusoids (about 10–15 μm in diameter) are also quite 'big' considering the size of a water molecule. Water molecules may be freer to move inside *in vivo* tissue than we anticipated.

As ADC measure is heavily affected by T2 (6), in addition to minimizing the perfusion information, one of the goals of using SDC is also to minimize the T2 effect. For tissues with T2 less than 70 ms (such as spleen and HCC), the advantage of SDC over ADC has been demonstrated (*Figures 6*,7). For these tissues' ADC, we consider them to be '*fast diffusion compartment dominant*', and longer T2 depresses the measure for ADC's '*fast diffusion compartment*' (6). By focusing on the '*slow diffusion compartment*', SDC measured higher values for the spleen and HCC than for the liver. This is likely to reflect truly faster '*slow diffusion*' of the spleen and HCC than that of the liver. For tissues with T2 of more than 80 ms (such as cyst), longer T2 promotes the measure for ADC's '*slow diffusion compartment*' (6). For SDC, despite cysts having longer T2 than hemangiomas (*Figure 3*), $SDC_{hemangioma}$ was higher than SDC_{cyst}, thus SDC is not dominated by the T2 effect. The T2 effect would ever exist, but this might be further mitigated by only using a small to moderate interval between the high *b*-value and the higher *b*-value for SDC calculation. Note that liver hemangiomas have a very high DDVD measure while the DDVD of liver cysts is close to zero when properly measured (14,32).

As the liver has a rather short T2, DW images of the liver with higher *b*-values are commonly associated with a low signal-to-noise ratio. This study used historical liver IVIM data, and we did not purposely try to optimize image quality with high *b*-values. For the absolute SDC values, the 95% confidence intervals as shown in *Figure* 7 were overall large. This is partly due to some of the lesion sizes being small. *Figure* 7 also shows absolute SDC values from different scanners/different magnetic fields may not be directly comparable. In our study, TE for 1.5T acquisition (=63 ms) and for 3.0T acquisition (=59 ms) are slightly different. A small but anticipated difference in Δ (time interval between the two motion probing pulses) and δ (time duration of the motion probing pulses) among different scanner models might also have contributed to the absolute SDC value difference between 1.5T results and 3.0T results. Our earlier experience with DDVD is that the ratio results were more comparable (14), and this is also tentatively shown in *Figure 6*. For DDVD-based differential diagnosis with the same MRI scanner, DDVD ratio results have been shown to be 'somewhat' better, but not massively better, than absolute DDVD values at a group level (33-35).

In this study, we tested whether ADC values calculated using Eq. [3] but with various combinations of high *b*-values could play a similar role as SDC. However, with all the combinations of liver DWI clinically applicable *b*-values as shown in *Figure 12*, spleen ADCs were all lower than liver ADCs. Therefore, ADC value calculated with a combination of high *b*-values cannot replace SDC. The literature results of IVIM-D_{slow} also differ from SDC. IVIM-D_{slow} and IVIM-PF for the spleen have been consistently measured much lower than that of the liver (15). In most literature reports, IVIM-D_{slow} for HCC has been measured lower than that of the surrounding liver parenchyma (36-38). Therefore, IVIM-D_{slow} also cannot replace SDC. Note that, though in principle SDC and IVIM-D_{slow} measure the same phenomenon, the actual calculation approaches are different. In its most simplified term, IVIM-D_{slow} is calculated according to:

$$IVIM\text{-}D_{slow} = \frac{S(b_{200})/S(b_0) - S(b_{600})/S(b_0)}{b_{600} - b_{200}} \left[unit: mm^2/s\right] \quad [4]$$

$S(b_0)$ is affected by T2 of the target tissues. Therefore, the compounding factor of $S(b_0)$ is introduced. Though histology and imaging data such as those of perfusion CT and DDVD show HCCs tend to be hypervascular, in most IVIM literature, PF for HCC has been reported to be lower than PF of the adjacent liver (33,36,38). For IVIM analysis excluding b=0 s/mm^2 data, as such when curving fitting starts from b=2 s/mm^2, IVIM results are still heavily affected T2 (39). It has also been described that IVIM analysis poorly characterizes liver hemangioma (40).

There are many limitations to this study. The assumptions of: (I) the spleen has a faster diffusion than the liver; (II) HCC has a faster diffusion than the surrounding liver parenchyma; and (III) liver hemangioma has a faster diffusion than liver cyst, are all based on theorization, rather than actual experimental validation. While MRI perfusion measures can be validated such as the results in *Figure 2* and the liver IVIM-PF being approximately 20% (15,36), diffusion measures cannot be validated (41). This study aimed only to prove the principle that the spleen and

HCC have a faster diffusion than liver parenchyma, and hemangiomas have a faster diffusion than the simple liver cysts, while we did not pre-calculate the statistical power for significance of among various entities' SDC. For the 3.0T data ratio difference of $SDC_{hemangioma}/SDC_{liver}$ and SDC_{cyst}/SDC_{liver}, the P value was only 0.096. However, we highly anticipate that, given sufficient sample size, the observed trend will be statistically significant. For the patient studies with HCC, potential variability such as liver fibrosis will affect ratios. The primary goal of this study was not to recommend the wider adoption of the diffusion metric SDC, which will require more testing with various organs and with different pathological entities. Data acquisition optimization for SDC also remains to be further explored. How SDC is sensitive to the TE parameter, as compared with that of ADC, should be explored in future studies. We also anticipate that further improvement of DWI data acquisition techniques will enhance the stability of DDVD and SDC measurement.

Conclusions

In conclusion, with the diffusion metrics SDC, in this study we achieved our primary goal of confirming that, the spleen has a faster diffusion than the liver, HCC tumorous tissues on average have a faster diffusion than the surrounding liver parenchyma, and hemangiomas have a faster diffusion than the simple liver cysts. There is a possibility that SDC will be a useful diffusion metric in clinical practice. Theoretically, an application of four DWI *b*-values, such as *b*=0, 10, 600, 800 s/mm^2, will allow the generation of three parameters, i.e., DDVD, SDC, and ADC, with ADC considered a composite biomarker commonly dominated by T2 effect and with its features in various disease entities well characterized. This may further improve disease classifications.

Acknowledgments

None.

Footnote

Funding: This study received funding from a Hong Kong GRF Project (No. 14112521).

Conflicts of Interest: All authors have completed the ICMJE uniform disclosure form (available at https://qims.amegroups.com/article/view/10.21037/qims-2025-537/coif). Y.X.J.W. serves as the Editor-in-Chief of *Quantitative Imaging in Medicine and Surgery*. Y.X.J.W. is the founder of Yingran Medicals Ltd., which develops medical image-based diagnostics software. B.H.X. contributed to the development of Yingran Medicals Ltd. The other author has no conflicts of interest to declare.

Ethical Statement: The authors are accountable for all aspects of the work in ensuring that questions related to the accuracy or integrity of any part of the work are appropriately investigated and resolved. This is a retrospective analysis of previously prospectively acquired liver IVIM data. The study was conducted in accordance with the Declaration of Helsinki (as revised in 2013). All IVIM data were acquired with institutional ethical approval and with informed consent obtained from individual participants.

References

1. Wáng YXJ, Zhao KX, Ma FZ, Xiao BH. The contribution of T2 relaxation time to MRI-derived apparent diffusion coefficient (ADC) quantification and its potential clinical implications. Quant Imaging Med Surg 2023;13:7410-6.
2. Wáng YXJ, Ma FZ. A tri-phasic relationship between T2 relaxation time and magnetic resonance imaging (MRI)-derived apparent diffusion coefficient (ADC). Quant Imaging Med Surg 2023;13:8873-80.
3. Wáng YXJ. The very low magnetic resonance imaging apparent diffusion coefficient (ADC) measure of abscess is likely due to pus's specific T2 relaxation time. Quant Imaging Med Surg 2023;13:8881-5.
4. Wáng YXJ, Aparisi Gómez MP, Ruiz Santiago F, Bazzocchi A. The relevance of T2 relaxation time in interpreting MRI apparent diffusion coefficient (ADC) map for musculoskeletal structures. Quant Imaging Med Surg 2023;13:7657-66.

5. Wáng YXJ. Natural course of apparent diffusion coefficient (ADC) change after brain ischemic stroke: an alternative explanation by the triphasic relationship between T2 and ADC. Quant Imaging Med Surg 2024;14:9848-55.
6. Wáng YXJ. An explanation for the triphasic dependency of apparent diffusion coefficient (ADC) on T2 relaxation time: the multiple T2 compartments model. Quant Imaging Med Surg 2025;15:3779-91.
7. Lutsep HL, Albers GW, DeCrespigny A, Kamat GN, Marks MP, Moseley ME. Clinical utility of diffusion-weighted magnetic resonance imaging in the assessment of ischemic stroke. Ann Neurol 1997;41:574-80.
8. DeMulder D, Ascher SM. Uterine Leiomyosarcoma: Can MRI Differentiate Leiomyosarcoma From Benign Leiomyoma Before Treatment? AJR Am J Roentgenol 2018;211:1405-15.
9. Bura V, Pintican RM, David RE, Addley HC, Smith J, Jimenez-Linan M, Lee J, Freeman S, Georgiu C. MRI findings in-between leiomyoma and leiomyosarcoma: a Rad-Path correlation of degenerated leiomyomas and variants. Br J Radiol 2021;94:20210283.
10. Barral M, Placé V, Dautry R, Bendavid S, Cornelis F, Foucher R, Guerrache Y, Soyer P. Magnetic resonance imaging features of uterine sarcoma and mimickers. Abdom Radiol (NY) 2017;42:1762-72.
11. Wáng YXJ. Living tissue intravoxel incoherent motion (IVIM) diffusion MR analysis without b=0 image: an example for liver fibrosis evaluation. Quant Imaging Med Surg 2019;9:127-33.
12. Xiao BH, Huang H, Wang LF, Qiu SW, Guo SW, Wáng YXJ. Diffusion MRI Derived per Area Vessel Density as a Surrogate Biomarker for Detecting Viral Hepatitis B-Induced Liver Fibrosis: A Proof-of-Concept Study. SLAS Technol 2020;25:474-83.
13. Ma FZ, Xiao BH, Wáng YXJ. MRI signal simulation of liver DDVD (diffusion derived 'vessel density') with multiple compartments diffusion model. Quant Imaging Med Surg 2025;15:1710-8.
14. Ju ZG, Leng XM, Xiao BH, Sun MH, Huang H, Hu GW, Zhang G, Sun JH, Zhu MSY, Guglielmi G, Wáng YXJ. Influences of the second motion probing gradient b-value and T2 relaxation time on magnetic resonance diffusion-derived 'vessel density' (DDVD) calculation: the examples of liver, spleen, and liver simple cyst. Quant Imaging Med Surg 2025;15:74-87.
15. Yu WL, Xiao BH, Ma FZ, Zheng CJ, Tang SN, Wáng YXJ. Underestimation of the spleen perfusion fraction by intravoxel incoherent motion MRI. NMR Biomed 2023;36:e4987.
16. Greenway CV, Stark RD. Hepatic vascular bed. Physiol Rev 1971;51:23-65.
17. Wáng YXJ, Li CY, Yao DQ, Tang SN, Xiao BH. The impacts of time of echo (TE) and time of repetition (TR) on diffusion-derived 'vessel density' (DDVD) measurement: examples of liver, spleen, and hepatocellular carcinoma. Quant Imaging Med Surg 2025;15:3771-8.
18. Yao DQ, King AD, Zhang R, Xiao BH, Wong LM, Wáng YXJ. Assessing parotid gland tumor perfusion with a new imaging biomarker DDVD (diffusion-derived vessel density): promising initial results. Rofo 2025. [Epub ahead of print]. doi: 10.1055/a-2543-3305.
19. Martirosian P, Boss A, Deimling M, Kiefer B, Schraml C, Schwenzer NF, Claussen CD, Schick F. Systematic variation of off-resonance prepulses for clinical magnetization transfer contrast imaging at 0.2, 1.5, and 3.0 tesla. Invest Radiol 2008;43:16-26.
20. Kapila V, Wehrle CJ, Tuma F. Physiology, Spleen. 2025.
21. Yeung J, Sivarajan S, Treibel TA, Rosmini S, Fontana M, Gillmore JD, Hawkins PN, Punwani S, Moon JC, Taylor SA, Bandula S. Measurement of liver and spleen interstitial volume in patients with systemic amyloid light-chain amyloidosis using equilibrium contrast CT. Abdom Radiol (NY) 2017;42:2646-51.
22. Yamada I, Aung W, Himeno Y, Nakagawa T, Shibuya H. Diffusion coefficients in abdominal organs and hepatic lesions: evaluation with intravoxel incoherent motion echo-planar MR imaging. Radiology 1999;210:617-23.
23. Parikh T, Drew SJ, Lee VS, Wong S, Hecht EM, Babb JS, Taouli B. Focal liver lesion detection and characterization with diffusion-weighted MR imaging: comparison with standard breath-hold T2-weighted imaging. Radiology 2008;246:812-22.
24. Tokgoz O, Unlu E, Unal I, Serifoglu I, Oz I, Aktas E, Caglar E. Diagnostic value of diffusion weighted MRI and ADC in differential diagnosis of cavernous hemangioma of the liver. Afr Health Sci 2016;16:227-33.
25. Erturk SM, Ichikawa T, Kaya E, Yapici O, Ozel A, Mahmutoglu AS, Basak M. Diffusion tensor imaging of cysts, hemangiomas, and metastases of the liver. Acta Radiol 2014;55:654-60.
26. Fenlon HM, Tello R, deCarvalho VL, Yucel EK. Signal characteristics of focal liver lesions on double echo T2-weighted conventional spin echo MRI: observer performance versus quantitative measurements of T2 relaxation times. J Comput Assist Tomogr 2000;24:204-11.
27. Cittadini G, Santacroce E, Giasotto V, Rescinito G. Focal

liver lesions: characterization with quantitative analysis of T2 relaxation time in TSE sequence with double echo time. Radiol Med 2004;107:166-73.
28. Cieszanowski A, Szeszkowski W, Golebiowski M, Bielecki DK, Grodzicki M, Pruszynski B. Discrimination of benign from malignant hepatic lesions based on their T2-relaxation times calculated from moderately T2-weighted turbo SE sequence. Eur Radiol 2002;12:2273-9.
29. Nam SJ, Park KY, Yu JS, Chung JJ, Kim JH, Kim KW. Hepatic cavernous hemangiomas: relationship between speed of intratumoral enhancement during dynamic MRI and apparent diffusion coefficient on diffusion-weighted imaging. Korean J Radiol 2012;13:728-35.
30. Egnell L, Jerome NP, Andreassen MMS, Bathen TF, Goa PE. Effects of echo time on IVIM quantifications of locally advanced breast cancer in clinical diffusion-weighted MRI at 3 T. NMR Biomed 2022;35:e4654.
31. Führes T, Riexinger AJ, Loh M, Martin J, Wetscherek A, Kuder TA, Uder M, Hensel B, Laun FB. Echo time dependence of biexponential and triexponential intravoxel incoherent motion parameters in the liver. Magn Reson Med 2022;87:859-71.
32. Hu GW, Li CY, Zhang G, Zheng CJ, Ma FZ, Quan XY, Chen W, Sabarudin A, Zhu MSY, Li XM, Wáng YXJ. Diagnosis of liver hemangioma using magnetic resonance diffusion-derived vessel density (DDVD) pixelwise map: a preliminary descriptive study. Quant Imaging Med Surg 2024;14:8064-82.
33. Li XM, Yao DQ, Quan XY, Li M, Chen W, Wáng YXJ. Perfusion of hepatocellular carcinomas measured by diffusion-derived vessel density biomarker: Higher hepatocellular carcinoma perfusion than earlier intravoxel incoherent motion reports. NMR Biomed 2024;37:e5125.
34. Lu BL, Yao DQ, Wáng YXJ, Zhang ZW, Wen ZQ, Xiao BH, Yu SP. Higher perfusion of rectum carcinoma relative to tumor-free rectal wall: quantification by a new imaging biomarker diffusion-derived vessel density (DDVD). Quant Imaging Med Surg 2024;14:3264-74.
35. Li CY, Chen L, Ma FZ, Chen JQ, Zhan YF, Wáng YXJ. High performance of the diffusion magnetic resonance imaging biomarker diffusion-derived 'vessel density' (DDVD) for separating placentas associated with pre-eclampsia from placentas in normal pregnancy. Quant Imaging Med Surg 2025;15:1-14.
36. Li YT, Cercueil JP, Yuan J, Chen W, Loffroy R, Wáng YX. Liver intravoxel incoherent motion (IVIM) magnetic resonance imaging: a comprehensive review of published data on normal values and applications for fibrosis and tumor evaluation. Quant Imaging Med Surg 2017;7:59-78.
37. Yue X, Lu Y, Jiang Q, Dong X, Kan X, Wu J, Kong X, Han P, Yu J, Li Q. Application of Intravoxel Incoherent Motion in the Evaluation of Hepatocellular Carcinoma after Transarterial Chemoembolization. Curr Oncol 2022;29:9855-66.
38. Ma FZ, Wáng YXJ. T(2) relaxation time elongation of hepatocellular carcinoma relative to native liver tissue leads to an underestimation of perfusion fraction measured by standard intravoxel incoherent motion magnetic resonance imaging. Quant Imaging Med Surg 2024;14:1316-22.
39. Xiao BH, Wáng YXJ. Different tissue types display different signal intensities on b = 0 images and the implications of this for intravoxel incoherent motion analysis: Examples from liver MRI. NMR Biomed 2021;34:e4522.
40. Wáng YXJ, Sabarudin A. Underestimation of liver hemangioma perfusion fraction by standard intravoxel incoherent motion diffusion magnetic resonance imaging. Quant Imaging Med Surg 2024;14:2128-35.
41. Le Bihan D, Turner R, Moonen CT, Pekar J. Imaging of diffusion and microcirculation with gradient sensitization: design, strategy, and significance. J Magn Reson Imaging 1991;1:7-28.

Cite this article as: Xu FY, Xiao BH, Wáng YXJ. The rationale for proposing a magnetic resonance slow diffusion metric and its proof-of-concept testing showing spleen parenchyma and hepatocellular carcinoma have faster diffusion than liver parenchyma. Quant Imaging Med Surg 2025;15(5):3792-3806. doi: 10.21037/qims-2025-537

